catalysts

MDPI

Article

Cobalt Catalyzed Fischer-Tropsch Synthesis with O_2-Containing Syngas

Alexander Herbers *, Christoph Kern and Andreas Jess

Chair of Chemical Engineering, Center of Energy Technology, University of Bayreuth, 95447 Bayreuth, Germany
* Correspondence: alexander.herbers@uni-bayreuth.de; Tel.: +49-921-55-7431

Abstract: Provision of sustainable transportation fuels is required for the energetic transition. A new process is presented for the production of synthetic sulfur free maritime fuel. This fuel is produced by Co-catalyzed Fischer-Tropsch synthesis (FTS) using syngas based on a plasma technology that contains traces of O_2. Gravimetric experiments and steady state measurements with a $Co/Pt/Al_2O_3$ catalyst at low temperature FTS conditions (10–30 bar, 180–230 °C) show that, with H_2 present in the system, the catalyst remains active for FTS, and shows no influence on the distribution of C_{2+}-hydrocarbons. O_2 is only converted to H_2O and CO_2 in varying proportions (H_2O: 70–80%, CO_2: 20–30%), whereby a higher CO concentration increases the CO_2 selectivity. This work may wield a new CO_2 source for carbon-neutral fuels.

Keywords: Fischer-Tropsch synthesis; maritime fuel; oxygen; cobalt catalyst

Citation: Herbers, A.; Kern, C.; Jess, A. Cobalt Catalyzed Fischer-Tropsch Synthesis with O_2-Containing Syngas. *Catalysts* **2023**, *13*, 391. https://doi.org/10.3390/catal13020391

Academic Editors: Ning Rui and Lili Lin

Received: 23 December 2022
Revised: 2 February 2023
Accepted: 6 February 2023
Published: 10 February 2023

1. Introduction

Many efforts have been made to mitigate CO_2 emissions contributing to climate change. Nevertheless, the CO_2 output is currently still rising, mainly driven by a huge fossil fuel demand [1–4]. Therefore, the need for alternative energy resources in all sectors of the world's economy is imperative, above all in transportation, which today almost completely relies on oil-derived fuels such as gasoline, diesel/marine oil, and jet fuel.

The supply of the required electrical energy by renewables seems to be in principle possible on the long run, but their availability is fluctuating, and storage solutions are essential for a successful transformation of the current energy infrastructure mainly based on fossil fuels to a supply by renewables. Therefore, energy storage via chemicals is an important focus of today's energy research. Especially the power-to-liquid (PtL) approach yielding synthetic liquid fuels attracts attention both in industry and academia [5–7].

Long-distance travel by ship or airplanes depends on fuels with a high gravimetric and volumetric energy density such as liquid hydrocarbons, and their substitution by battery electric or hydrogen fuel cell driven systems is not viable [8,9]. Hence, synthetic liquid fuels providing the required energy density will be needed to reduce the CO_2 emissions related to transportation by air and shipping [10,11]. In particular, the maritime sector is strongly looking for an alternative fuel. As the cargo-shipping business is highly competitive, transportation costs are important. As a result, the shipping companies today rely on heavy bunker oil which is low in price but also low in quality, i.e., the fuel contains high amounts of organic sulfur and nitrogen compounds, which leads to high emissions of SO_x, NO_x, and soot [12]. In order to solve this problem, the International Shipping Organization ruled new emission limits for maritime fuel. As the current fossil-based heavy oils by far do not meet these criteria, other kinds of fuels become attractive [11]. Considering that a whole infrastructure based on hydrocarbon fuels already exsists, the use of synthetic fuels as a substitute for heavy bunker oil is regarded as very promising [13].

Although the main problem with fossil fuels is the output of carbon dioxide, CO_2 can be beneficial for other processes. The direct capture of carbon dioxide from large

industrial plants with high CO_2 pollution, like steel mills and cement production, or the use of CO_2 formed as by-product in the chemical industry (e.g., NH_3 synthesis) can prevent—to a certain extent—the increase in atmospheric CO_2 and may serve as a carbon source for energy storage via synthetic fuels [10]. When direct capture of CO_2 and H_2O electrolysis (to provide H_2) based on renewable electricity (wind, hydro, solar) are joined skillfully, a Fischer-Tropsch plant can be operated to produce various green synthetic fuels, above all jet and maritime fuel. The latter is a mixture of long-chain linear hydrocarbons, thus low-temperature Co-catalyzed Fischer-Tropsch synthesis (LT-FTS) is the best choice for production [14]. Here, a multi-tubular fixed-bed reactor cooled by boiling water is typically used.

In a joint project of MCT Transformatoren GmbH, Overspeed GmbH, Institute for Photovoltaics of the University of Stuttgart, and the Chair of Chemical Engineering of the University of Bayreuth, such a process has been investigated. A process scheme is shown in Figure 1.

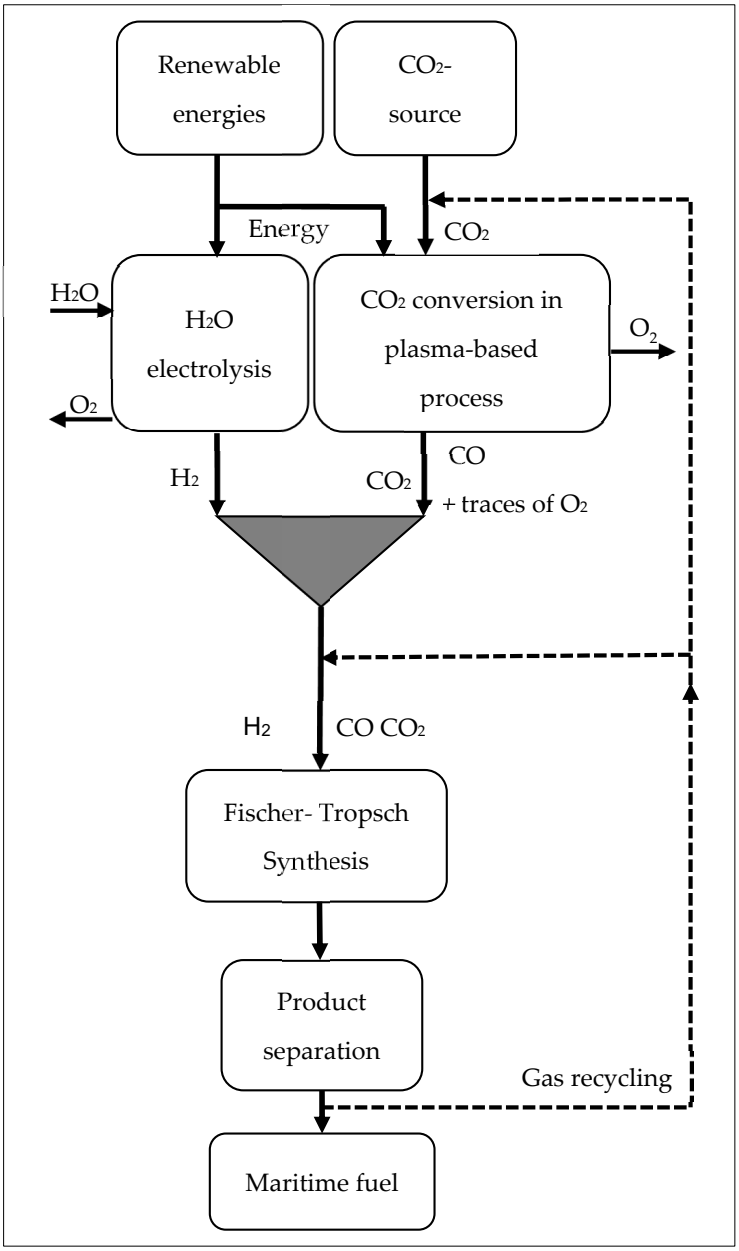

Figure 1. CO_2 capture and usage in Fischer-Tropsch Synthesis to produce maritime fuel.

In this process (Figure 1), CO_2 and H_2O are converted in one step to CO and H_2 by renewable electrical energy in a plasma-based CO_2 conversion combined with H_2O electrolysis, respectively, finally yielding the syngas needed for FTS; for details, see [15,16]. In this route, O_2 occurs as byproduct of the plasma process and can not be completely removed. Hence, FTS must be run with syngas containing traces of molecular O_2 (up to 2 vol.%) [15,16]. An alternative would be the catalytic conversion of oxygen with H_2 or CO in an upstream reactor, as also discussed below.

As only about 20% of the CO_2 is converted in the plasma process to CO per pass, CO_2 remains in the syngas as well. Previous works show that only for a high CO_2 concentration combined with a very low CO concentration carbon dioxide does affect the FTS—if cobalt is used as catalyst—otherwise, CO_2 acts as inert [17]. The latter is the case here. As seen in Figure 1, syngas is converted in the FTS unit to maritime fuel (and lighter hydrocarbons). Unconverted syngas and short chained hydrocarbons (such as C_1–C_4) are recycled into the plasma reactor to increase the overall CO_2 conversion to maritime fuel. The oxygen from the syngas production can be used in other industrial chemical processes such as the partial oxidation of methanol to formaldehyde [18].

Because no data exists for this process, the following questions had to be answered in this work with regard to the oxygen present in the syngas:

- Does the FT catalyst remain active for FTS in the presence of O_2?
- If the answer of 1. is yes, does the product composition of the FTS change?
- Where does the O_2 end up (selectivity to H_2O and CO_2)?
- What has to be considered in terms of process/FTS reactor safety?

In this work, the focus is on the general influence of oxygen and not on details of the consequences with regard to the detailed design and runaway aspects of an FT reactor.

The reaction scheme (Equations (1)–(4)) suggests that O_2 present in the feed gas only ends up in CO_2 and H_2O during FTS, but the possible oxidation of cobalt to CoO (not active for FTS [19]) is still also an issue. As CO_2 and H_2O do not affect the FTS reaction with Co as catalyst, at least an unwanted—but here unavoidable—loss of syngas (H_2, CO) occurs [14].

$$2\,H_2 + CO \rightarrow (\text{-}CH_2\text{-}) + H_2O_{(g)} \quad \Delta_R H_0^{298} = -152\ \text{kJ mol}^{-1} \tag{1}$$

$$3\,H_2 + CO \rightleftharpoons CH_4 + H_2O_{(g)} \quad \Delta_R H_0^{298} = -206\ \text{kJ mol}^{-1} \tag{2}$$

$$2\,H_2 + O_2 \rightarrow 2\,H_2O_{(g)} \quad \Delta_R H_0^{298} = -484\ \text{kJ mol}^{-1} \tag{3}$$

$$2\,CO + O_2 \rightarrow 2\,CO_2 \quad \Delta_R H_0^{298} = -566\ \text{kJ mol}^{-1} \tag{4}$$

With regard to thermodynamics, O_2 is favourably converted with CO to CO_2, e.g., for a syngas consisting of 1% O_2, 66% H_2, and 33% CO and typical FT conditions (30 bar, 230 °C); hence, the selectivity to CO_2 is ca. 99% with regard to thermodynamics. However, this value may not be reached with regard to reaction kinetics, as under stoichiometric FT conditions, the H_2 concentration exceeds the CO concentration twofold.

To our knowledge, the use of O_2-containing syngas in Fischer-Tropsch synthesis has never been considered before. Since this would expand the use of FTS to a syngas from new sources, it is a very important finding that we present. The results presented herein show a new power-to-liquid approach with a highly interesting syngas source and the possibilty to use CO_2 for maritime fuel production.

2. Results and Discussion

2.1. Stability of the FT Co Catalyst against O_2 in O_2-Containing Gas Mixtures

At first, the stability of the activated (reduced) FT Co catalyst was studied in different O_2-containing gas mixtures. Since cobalt is only active for FTS in metallic state [20,21], the crucial question was whether Co remains metallic or is oxidized. Hence, the catalyst's mass was monitored by a magnetic suspension balance (MSB). For example, a complete oxidation of cobalt to CoO would lead to an increase in the catalyst's mass (with 10 wt.% Co) by

2.7%. Two feed gases were initially used, 99% N_2/1% O_2 and 39% N_2/60% H_2/1% O_2; a typical FT temperature of 230 °C was thereby applied. H_2 is expected to hinder the oxidation of Co as only a small amount of O_2 (1%) is present in the feed gas. During these experiments, no CO was added to avoid FTS to take place, as this leads to an increase in the catalyst's mass by filling of pores with higher hydrocarbons, which would falsify the signal of the MSB. Thus, only the reaction of O_2 with H_2 to H_2O and/or the oxidation of Co was measured. For comparison, the catalyst mass was also observed in a 1% H_2O/99% N_2 mixture. After contact with one of the three gases, the catalyst batches were dried in pure N_2 followed by pure H_2; the initial temperature of 230 °C was thereby finally increased to 360 °C. Experimental details are given in Section 3.1. The results are shown in Figure 2.

In case of the O_2-containing but H_2-free feed gas (Figure 2a), a fast (relative) increase in the weight of the catalyst by 2.4% is observed at 230 °C. No O_2 conversion was detected via the gas analyzer. Switching to pure N_2 at 230 °C leaves the catalyst mass unaffected and only a small decrease is observed after rising the temperature to 360 °C. This implies that the mass increase is caused by the oxidation of Co. Previous investigations have shown that in a H_2 atmosphere, temperatures $\geq$ 360 °C are required to activate (reduce) the catalyst [22]. Therefore, cooling the reactor to 230 °C and changing from N_2 to H_2 does not decrease the catalyst's mass whereas the initial weight, i.e., the previous achieved reduction degree, is finally reached after several hours at 360 °C. Thus, the catalyst is oxidized if O_2 is present without a reducing agent, which is expected since formation of cobalt oxides (CoO) is then favorable. The Co dispersion on the surface was determined to 10% [22]. If only cobalt atoms directly exposed to the feed gas react with O_2, oxidation of cobalt to CoO at the surface would lead to a mass increase of only about 0.3%. Hence, the experimentally found value of 2.4% indicates that practically all Co atoms and not only the surface atoms are oxidized in an O_2-containing feed, if H_2 is not present. XRD measurements support this conclusion, showing the formation of only CoO in a H_2-free O_2-containing feed at elevated temperature and pressure (see Figure S1 in the Supporting Information).

In Figure 2b, O_2 as well as H_2 are present in the feed gas. Again, the catalyst's mass increases. However, the mass increase by 1.2% at 230 °C is only half the value compared to case a. Furthermore, the initial catalyst mass is again achieved in pure N_2, if the temperature is increased to 360 °C (no change at 230 °C). Hence, adsorption (of H_2O) instead of Co oxidation obviously causes the increase in the mass of the catalyst in the presence of H_2 and O_2, and cobalt remains in its metallic form. During this experiment, the conversion of O_2 is constant (here about 50%). This is also a clear indication that H_2O is formed by H_2 and O_2 and then adsorbs on the catalyst; in case of Co oxidation, the conversion of O_2 would decline with time on stream, if cobalt is more and more fully oxidized. In order to prove this hypothesis, a 1% H_2O/99% N_2 gas mixture was passed over the reduced catalyst. Hence, this content of steam is the value resulting from the measured oxygen conversion of about 50% for an initial O_2 content of 1%. The weight gain of the catalyst was then also 1.2% (Figure 2c), confirming that the formed H_2O adsorbs on a Co/Pt/Al_2O_3 catalyst in a H_2/O_2/N_2 gas mixture. Moreover, the initial catalyst weight is again obtained by drying (desorption) in pure N_2 at 360 °C as in Figure 2b. Similar measurements at a lower temperature (165 °C) show the same trend supporting this explanation (see Table 1).

Table 1. Maximum weight change of FTS particle after exposure with different gas mixtures. Conditions: T = 165–360 °C; p = 10 bar; $\dot{V}_{total}$ = 13 L/h (NTP); p_{H_2} = 0–10 bar, p_{N_2} = 0–10 bar; p_{O_2} = 0–0.1 bar; p_{H_2O} = 0–0.1 bar; initial m_{cat} (Co/Pt/Al_2O_3) = 1 g.

	Case A: Rel. Weight Change in O_2	**Case B: Rel. Weight Change in H_2/O_2**	**Case C: Rel. Weight Change in H_2O**
Feed gas	99% N_2, 1% O_2	60% H_2, 39% N_2, 1% O_2	98% N_2, 2% H_2O
165 °C	+2.3%	+2.4%	+2.1%
230 °C	+2.5%	+1.2%	+1.1%

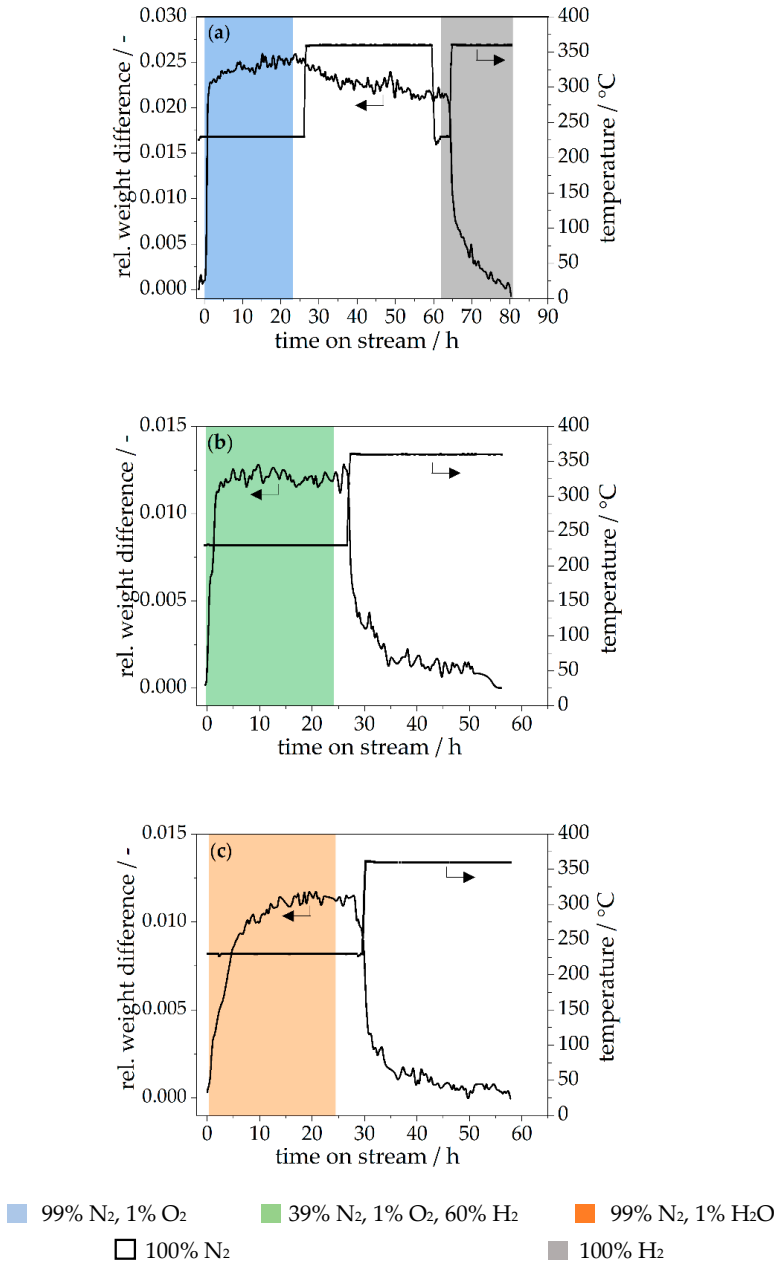

Figure 2. (**a**) Stability of catalyst in O_2-containing N_2 gas feed without H_2 present. (**b**) Stability of catalyst in O_2-containing N_2 gas feed with H_2 present. (**c**) Stability of catalyst in H_2O-containing N_2 gas feed (magnetic suspension balance). Conditions: T = 230–360 °C; p = 10 bar; $\dot{V}_{total}$ = 13 L/h (NTP); p_{H_2} = 0–10 bar, p_{N_2} = 0–10 bar; p_{O_2} = 0–0.1 bar; p_{H_2O} = 0–0.1 bar; m_{cat} (Co/Pt/Al_2O_3) = 0.5–1 g.

Table 1 summarizes the results: The weight gain caused by catalyst oxidation (case a) remains at around 2.5% at 165 °C, revealing that almost all cobalt atoms are then already oxidized to CoO. In case of a H_2/O_2 gas mixture (case b), the weight gain depends on temperature and is by a factor of two lower at 165 °C than at 230 °C. This trend also confirms H_2O adsorption (in a H_2/O_2 gas), as the (exothermic) adsorption is in general favored by a lower temperature. In both cases, the mass increase can be undone by drying in pure N_2 at 360 °C, confirming that the catalyst weight increase in a H_2/O_2 gas feed is due to surface adsorption of H_2O.

2.2. Reactivity of Co Catalyst for Fischer-Tropsch Synthesis with O_2-Containing Syngas

After the stability of Co against O_2 in the presence of H_2 was proven, the FTS was carried out with the Co/Pt/Al_2O_3-catalyst in O_2-containing syngas. The experiments with the fixed bed reactor were conducted to check whether O_2 prevents FTS or alters the product distribution. Initially, the FTS was run with O_2-free syngas (72 h). Then, syngas with 2% O_2 was used for further 72 h. Finally, O_2-free syngas was again used for 72 h to check if deactivation has occurred. The N_2 content was 23 or 25% to ensure constant partial pressures of H_2 and CO (ratio of 2) for a syngas with or without 2% O_2. In addition, the dilution with N_2 helps to ensure isothermal conditions, although numerous exothermic reactions may take place, see Equations (1)–(4). The results with regard to CO conversion and methane selectivity are shown in Figure 3.

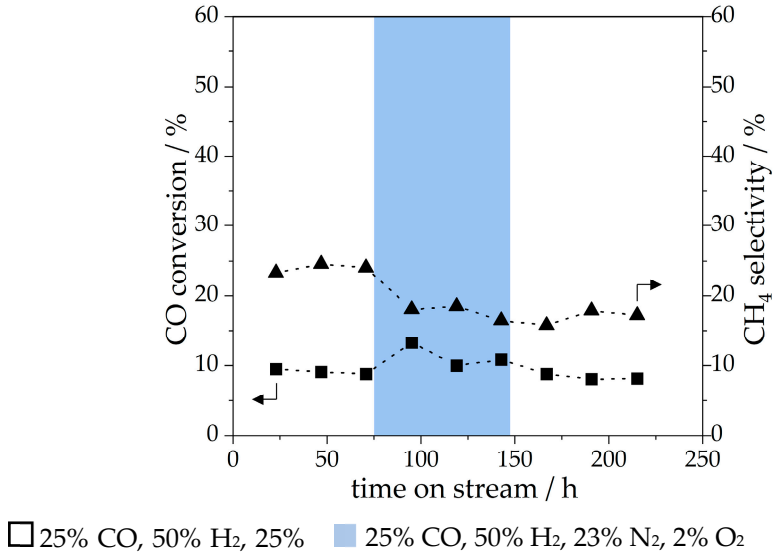

Figure 3. CO conversion and CH_4 selectivity during the FTS with and without O_2 in the syngas. Conditions: T = 225 °C; p = 20 bar; $\dot{V}_{total}$ = 7 L/h (NTP); p_{CO} = 5 bar; p_{H_2} = 10 bar, $p_{N_2+O_2}$ = 5 bar; m_{cat} (Co/Pt/Al_2O_3) = 1 g; X_{CO} = 0.09 (only FTS)–0.105 (with O_2); X_{O_2} = 0–0.4.

A constant CO conversion of 9% is reached for the first and third run (O_2-free syngas). Thus, the O_2 present in the second run does not lead to a change of the FT activity of the catalyst. In case of the O_2-containing syngas, the CO conversion is 10.5% and thus slightly higher compared to O_2-free syngas (9%), which can be attributed to the formation of CO_2 by reaction of CO with O_2. This is confirmed by the analysis of the produced hydrocarbons, which show no change of the product composition for an O_2-free or O_2-containing syngas. The O_2 conversion is 40%. Based on the amount of unconverted O_2 and formed CO_2 (determined based on each content detected via the gas analyzers downstream the reactor), it could be calculated that if all converted O_2 had reacted to CO_2, the CO conversion should have been 16% instead of the real value of 10.5% (for a CO feed content of 25%). In return, this leads to the conclusion that 21% of the converted O_2 is found in CO_2 (S_{CO_2} = 21%, S_{H_2O} = 79%).

The CH_4 selectivity decreases if O_2 (2%) is present in the syngas and drops from 24 to 16%. It does not return to the initial value, if syngas without O_2 is then again used (Figure 3). A reasonable explanation is adsorbed H_2O on the catalyst. According to Bertole, adsorbed H_2O leads to a decreased CO dissociation barrier and thereby to a higher hydrocarbon chain propagation rate due to more activated carbon [23], i.e., in return, to less methane formation. As H_2O stays adsorbed on the catalyst at the chosen temperature (see Figure 2c), this effect may still be present even if O_2 is no longer present in the feed gas. This effect, although rather small, is beneficial as a yield of higher hydrocarbons (HCs) and a lower yield of CH_4 are desired. Hence, more maritime fuel, i.e., C_{11+}-HCs, are obtained.

2.3. Selectivity of Reaction of Oxygen (to CO_2 or H_2O) If Present in the Syngas of FTS

Knowing that the FT catalyst is still active in O_2-containing syngas and that oxygen does not affect the FTS other than reducing to a small extent the CH_4 selectivity, the focus is subsequently on O_2 consumption and selectivity to CO_2 and H_2O, which turned out to be the only products. For a detailed understanding of the O_2 reaction, only the influence of the FTS had to be minimized: The FTS can have an influence because strongly exothermic reactions (Equations (1) and (2)) take place, and the conversion of CO by reaction of oxygen is hard to detect accurately, if conversion by FTS is dominating. Consequently, the CO conversion by FTS must be as low as possible, but the O_2 consumption rate also decreases with lower CO conversion, e.g., by a lower temperature or residence time. However, for example, for an O_2 conversion of about 20%, the CO conversion by FTS is then only around 2% (Figure 4). As a result, the selectivity of H_2O and CO_2 formation from O_2 could be determined more precisely as a function of temperature, pressure, and concentration of O_2, CO, and H_2.

At first, the temperature was varied. Figure 4a shows the reaction rate of CO (with and without 1% O_2), the rate of O_2 consumption, as well as the formation rate of CO_2; the corresponding selectivities to CO_2 and H_2O are also shown (Figure 4b). The adjusted O_2 conversion was about 20%.

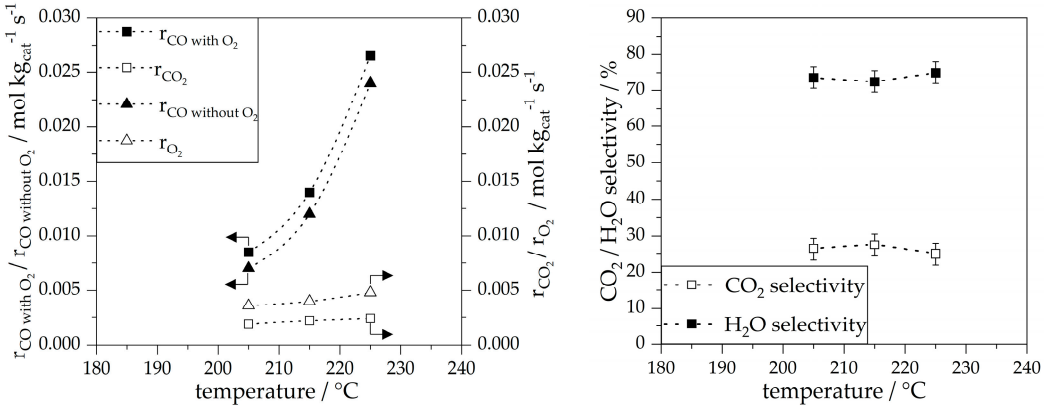

Figure 4. (**a**) Reaction rates of CO, CO_2, and O_2 during FTS with O_2-free and O_2-containing syngas. (**b**) H_2O and CO_2 selectivity of occurring O_2 consumption. Conditions: T = 205–225 °C; p = 20 bar; $\dot{V}_{total}$ = 11.5–18 L/h (NTP); p_{CO} = 5 bar; p_{H_2} = 10 bar, $p_{N_2+O_2}$ = 5 bar; m_{cat} (Co/Pt/Al_2O_3) = 1 g; X_{CO} = 0.01–0.02 (only by FTS); X_{O_2} = 0.2.

Figure 4a depicts that the increase in the CO reaction rate by addition of O_2 is always equivalent to the formation rate of CO_2. This again indicates that the FTS only is not affected by O_2: For temperatures between 205 and 225 °C, the CO rate varies from 0.87×10^{-2} to 2.65×10^{-2} mol kg_{cat}^{-1} s^{-1} in case of 1% O_2 in the syngas, and from 0.7×10^{-2} to 2.4×10^{-2} mol kg_{cat}^{-1} s^{-1} for an O_2-free syngas. The difference of the CO rates matches the rate of CO_2 formation (0.19×10^{-2} to 0.25×10^{-2} mol kg_{cat}^{-1} s^{-1}). The rate of O_2 consumption (0.36×10^{-2} to 0.5×10^{-2} mol kg_{cat}^{-1} s^{-1}) is much higher compared to the case of CO_2 formation only ($r_{CO_2} = 2\, r_{O_2}$), indicating that in the given temperature range, around 75% of O_2 are converted to H_2O (Figure 4b).

In order to check whether Co and/or Pt catalyzes the O_2 consumption, experiments were conducted with catalysts not containing Co or Pt. In both cases, the individual metal content was the same as of the standard FT catalyst (10 wt.% Co, 0.03 wt.% Pt). The experiments were carried out with an O_2-containing syngas (60% H_2, 30% CO, 9% N_2 and 1% O_2) at 20 bar and 180 °C; the O_2 conversion was held at 20% by variation of the residence time. In addition, the Al_2O_3 support (without Co and Pt) was also tested. The results are shown in Table 2. Each catalyst was tested with or without pre-treatment (reduction at 360 °C in pure H_2).

Table 2. Selectivity of O_2 reaction for different catalysts and the support material. Conditions: p = 20 bar; T = 180 °C; $\dot{V}_{total}$ = 7.5–75 L/h (NTP); p_{CO} = 6 bar; p_{H_2} = 12 bar, p_{N_2} = 1.8 bar; p_{O_2} = 0.2 bar; m_{cat} = 0.4–1.2 g; X_{O_2} = 0.2.

Catalyst	Pre-Reduction at 360 °C	Oxidation State of Co and Pt	r_{O_2} in mol_{O_2} kg_{cat}^{-1} s^{-1}	S_{CO_2} in %	S_{H_2O} in %
Al_2O_3	No	-	-	no O_2 conversion	
	Yes	-	-	no FTS-activity	
9.7 wt.% Co rest Al_2O_3	No	+2 (CoO)	0.3×10^{-2}	80 ± 3	20 ± 3
	Yes	+2 (CoO)	0.3×10^{-2}	80 ± 3	20 ± 3
0.03 wt.% Pt rest Al_2O_3	No	0 (Pt)	0.4×10^{-2}	58 ± 3	42 ± 3
	Yes	0 (Pt)	0.4×10^{-2}	58 ± 3	42 ± 3
10 wt.% Co, 0.03 wt.% Pt rest Al_2O_3	No	+2 (CoO), 0 (Pt)	0.7×10^{-2}	63 ± 3	37 ± 3
	yes, fresh catalyst	0 (Co), 0 (Pt)	3.5×10^{-2}	36 ± 3	64 ± 3
	yes, cat. In steady state (100 h TOS)	0 (Co), 0 (Pt)	0.2×10^{-2}	27 ± 3	73 ± 3

With the Al_2O_3 support, only no reaction (FTS or O_2-consumption) occurred (Table 2). If the catalyst containing only Co is used, FTS does not take place, and the CO_2 formation rate is four times faster than the H_2O formation, i.e., the selectivity to CO_2 is always 80%. Note that in this case, the pre-reduction does not lead to metallic Co, as Pt is needed as reduction promotor to convert CoO to Co at 360 °C, as confirmed by thermogravimetric analysis (see Figure S2 in Supporting Information) and also reported in [22]. This explains that FTS is suppressed as metallic Co is needed.

If only platinum on Al_2O_3 is used, the selectivity to CO_2 is always 58% (H_2O selectivity 42%), and the rate of O_2 consumption is then by a factor of 1.33 higher compared to the Co catalyst (without Pt). Again, the application of the pre-reduction does not influence the catalyst's activity as Pt is always in the metallic state. If the $Co/Pt/Al_2O_3$ catalyst is used without pre-reduction (hence we have CoO), the resulting O_2 consumption rate is higher compared to Pt only, which reflects the contribution of CoO to the rate of O_2 consumption.

If the $Co/Pt/Al_2O_3$ catalyst is pre-reduced at 360 °C, this leads to a reduction in CoO due to Pt as reduction promotor [22]. Then, the oxygen consumption rate is very high, e.g., by a factor of 5 compared to the same catalyst without pre-reduction. Hence, metallic Co is quite active for conversion of oxygen. The selectivity to CO_2 with the reduced Co/Pt catalyst is about 36%.

For steady-state conditions, reached after 100 h TOS, the pores of the catalyst are completely filled with liquid HCs [15], and the rate of O_2 consumption is then strongly reduced to only about 6% of the value reached at identical conditions with the fresh catalyst. Hence, the liquid higher hydrocarbons present in the pores obviously limit the oxygen transport to the catalyst surface and act as a protective layer.

2.4. Selectivity of O_2 Reaction in Steady-State Operation of Fischer-Tropsch Synthesis

The influence of the total pressure and of the O_2 content in the feed gas on oxygen consumption at a temperature of 215 °C is depicted in Figure 5. These measurements were conducted with the pre-reduced $Co/Pt/Al_2O_3$ catalyst under steady state conditions of FTS. Figure 5 reveals that both the influence of the O_2 content and of the total pressure on the selectivity to CO_2 and H_2O is small (Figure 5a).

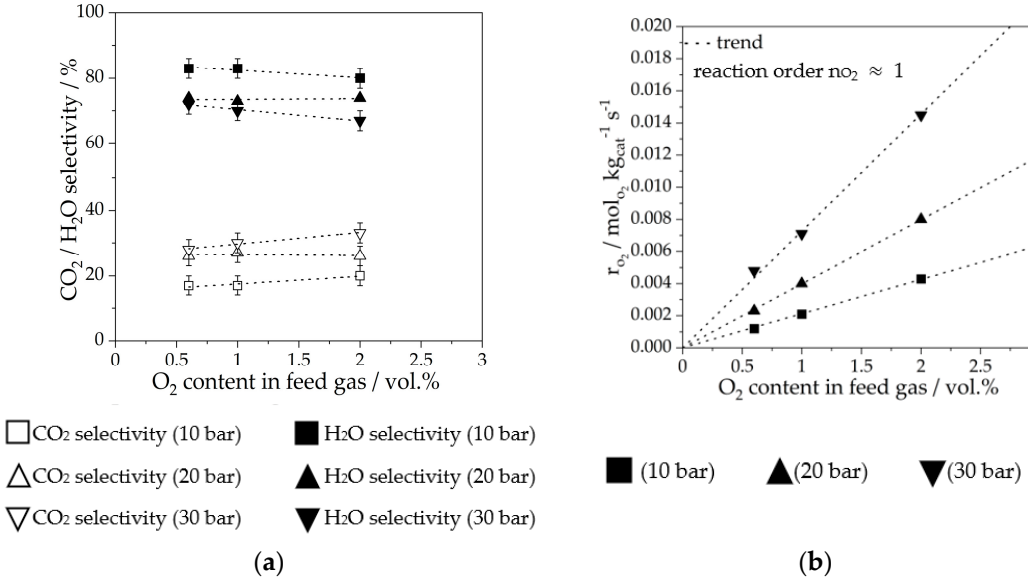

Figure 5. (**a**) CO_2/H_2O selectivity vs. O_2 concentration in the FTS with O_2-containing syngas. (**b**) O_2 consumption rate vs. O_2 concentration in the FTS with O_2-containing syngas. Conditions: T = 215 °C, p = 10–30 bar; $\dot{V}_{total}$ = 15.9 L/h (NTP); p_{CO} = 1.6–5 bar; p_{H_2} = 3.3–10 bar, $p_{N_2+O_2}$ = 5–15 bar; m_{cat} ($Co/Pt/Al_2O_3$) = 1 g; X_{CO} = 0.02; X_{O_2} = 0.2–0.25.

The O_2 reaction rate almost linearly increases with the O_2 content (at constant total pressure) and with pressure (at constant O_2 content) (Figure 5b). Hence, the rate is first order with regard to O_2. To investigate the influence of the H_2 and CO content on the O_2 consumption, the feed gas content of these two syngas components were varied individually while the concentration of the other component was kept constant by the respective content of N_2 in the syngas. Again, steady state FT conditions were applied (TOS > 100 h). The results (again at 215 °C) are presented in Figures 6 and 7. Both figures (cases a) show that the influence of the content of H_2 and of CO on the selectivity to CO_2 and H_2O is marginal or rather low, respectively: The CO_2 selectivity decreases from 30 to 27% for a variation of the H_2 content between 7 to 60% (Figure 6a). For CO, the increase in the content from 3 to 30% leads to an increase in the CO_2 selectivity from 21 to 33% (Figure 7a). For both gases, each content has no measurable influence on the consumption rate of O_2 (Figures 6b and 7b).

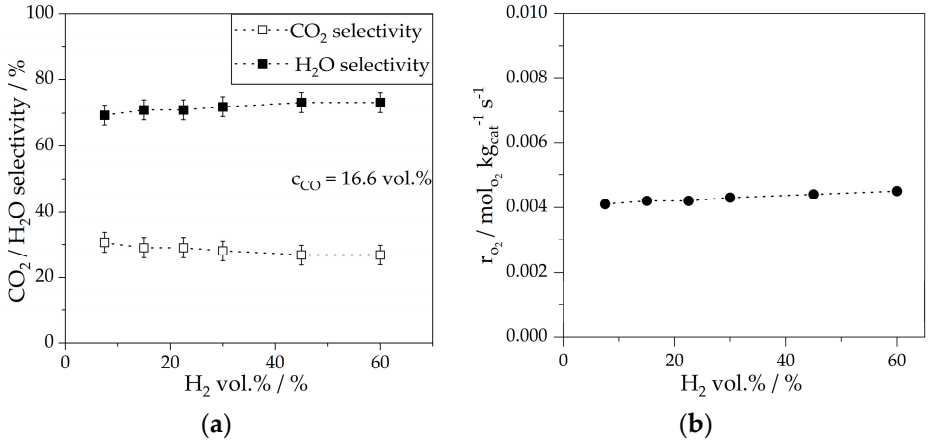

Figure 6. (**a**) Selectivity of O_2 products for different H_2 concentrations. (**b**) Oxygen reaction rate for different H_2 concentrations. Conditions: p = 20 bar; T = 215 °C; $\dot{V}_{total}$ = 15.9 L/h (NTP); p_{CO} = 3.3 bar; $p_{H_2+N_2}$ = 16.5 bar; p_{O_2} = 0.2 bar; m_{cat} ($Co/Pt/Al_2O_3$) = 1 g; X_{CO} = 0.02; X_{O_2} = 0.2.

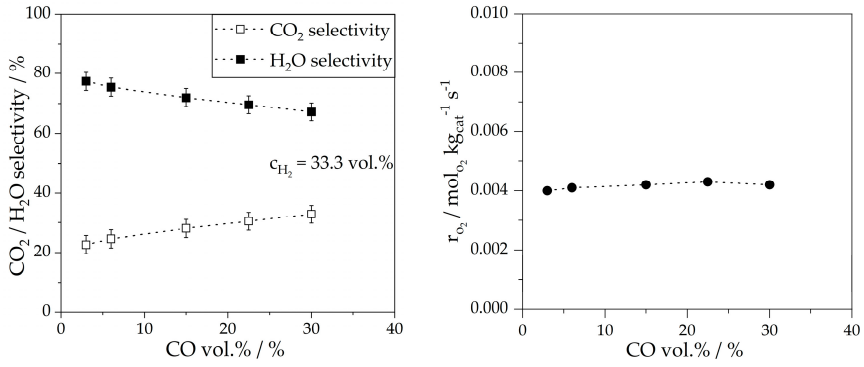

Figure 7. (**a**) Selectivity of O_2 products for different CO concentrations. (**b**) Oxygen reaction rate for different CO concentrations. Conditions: p = 20 bar; T = 215 °C; $\dot{V}_{total}$ = 15.9 L/h (NTP); p_{CO+N_2} = 13.2 bar; p_{H_2} = 6.6 bar; p_{O_2} = 0.2 bar; m_{cat} (Co/Pt/Al_2O_3) = 1 g; X_{CO} = 0.02; X_{O_2} = 0.2.

3. Materials and Methods

Two different sets of experiments were conducted to study the effect of oxygen on FTS: The change of mass of the catalyst was studied gravimetrical in a magnetic suspension balance. In addition, the activity and selectivity of the catalyst both for FTS and conversion of the oxygen present in the syngas (to either CO_2 or H_2O) were measured in a classical fixed bed reactor with and without O_2-containing syngas at temperatures typical for LT-FTS (180–230 °C).

3.1. Measurements in a Magnetic Suspension Balance

The setup of the gravimatrical measurements (Figure 8) consists of four individual gas supply lines for CO, H_2, N_2, and air, respectively. The flow of each gas is regulated by mass flow controllers (Bronkhorst F-201V, Bronkhorst High-Tech B.V., Ruurlo, The Netherlands). The measurements of the Co-based catalyst stability against O_2 were conducted in a magnetic suspension balance (MSB) (*TA Instruments* former *RUBOTHERM*, New Castle, DE, USA). The catalyst particles are put in a steel retainer inside the MSB; the MSB device is electrically heated, and the temperature is measured and controlled by a dual PT-100 thermocouple) (*TA Instruments* former *RUBOTHERM*, New Castle, DE, USA). Condensable products (i.e., higher hydrocarbons and H_2O) are collected in two serial cooling traps, one trap at room temperature and the other trap at 0 °C. The gas leaving the cooling traps passes through a gas analyzer (Emerson X-Stream Enhanced XEPG, Emerson Electric Company, St. Louis, MO, USA) and the gas flow is measured in a soap bubble flow meter at the outlet of the setup.

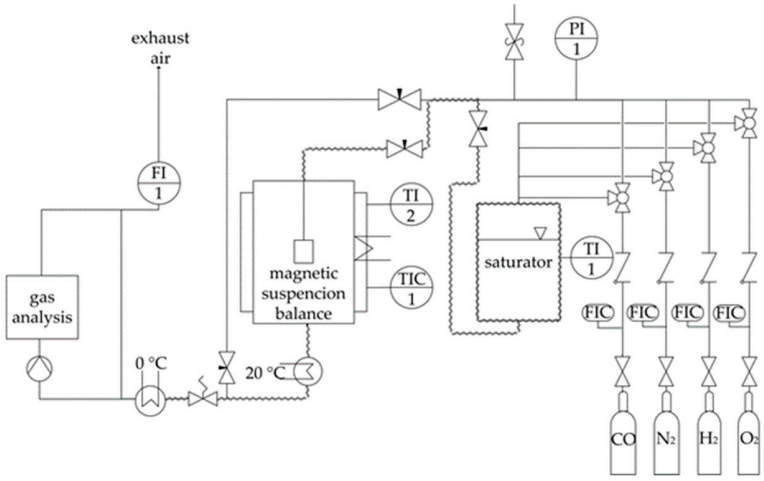

Figure 8. Setup of the magnetic suspension balance.

Prior to the FTS experiments, the cobalt catalyst is reduced and activated in pure H_2 for 16 h at 360 °C and then cooled to 100 °C. Thereafter, the partial pressures of the desired gases are adjusted, and the gas mixture passes through the MSB for 24 h at 165 °C or 230 °C. Afterwards, pure N_2 is introduced to remove adsorbed species from the catalyst surface. The desorption is performed in two steps. First, drying is conducted for at least 3 h under the chosen temperature, i.e., at either 165 °C or 230 °C, until the catalyst mass remains constant. Then, the reactor is heated up to the maximum temperature of 360 °C (5 K min^{-1}). The heating is stopped when the mass signal remains constant or the initial mass of the activated catalyst is restored. If the mass is still above the initial mass, the drying procedure is repeated, but instead of N_2 pure H_2 is used to reduce the catalyst until the initial mass is regained.

3.2. Fischer-Tropsch Synthesis

FTS experiments are conducted in a fixed-bed reactor. The mass flows of the reactant gases CO, H_2, N_2, and O_2 are supplied and controlled by mass flow controllers (Bronkhorst EL-Flow Prestige, Bronkhorst High-Tech B.V., Ruurlo, The Netherlands). The reactor is an electrical heated steel tube that is 600 mm in length and 15 mm in diameter; the packed catalyst bed has a height of 150 mm. A guiding tube in the center of the reactor (6 mm diameter) over the total length was used to measure the axial temperature profile by means of a movable thermocouple; for the given conditions, it turned out that the fixed bed could be regarded as isothermal. Figure 9 shows the setup for the FTS experiments.

The product gas stream passes through three cooling traps to collect the condensable products. These cooling traps are connected in series at 120 °C, room temperature, and 0 °C. The remaining gaseous products are analyzed by a GC (Perkin Elmer Clarus® 690 GC, PerkinElmer Inc., Waltham, MA, USA). In order to protect the following analytical device, a dry-ice-cooling trap is installed to remove the remaining water from the gas stream. The dry gas stream is analyzed (CO, CH_4, and CO_2 content) by an IR gas analyzer (Emerson X-Stream Enhanced Emerson Electric Company, St. Louis, MO, USA) and a paramagnetic oxygen sensor. Finally, the gas flow is measured via a gas meter (Ritter Apparatebau drum–type gas meter; type TG-5, Dr.-Ing. RITTER Apparatebau GmbH & Co. KG, Bochum, Germany) or a soap bubble flow meter. The collected condensable products are analyzed in a second GC (Bruker Varian CP-3800, Bruker Corporation, Billerica, MA, USA) in periodic time intervals during the reaction.

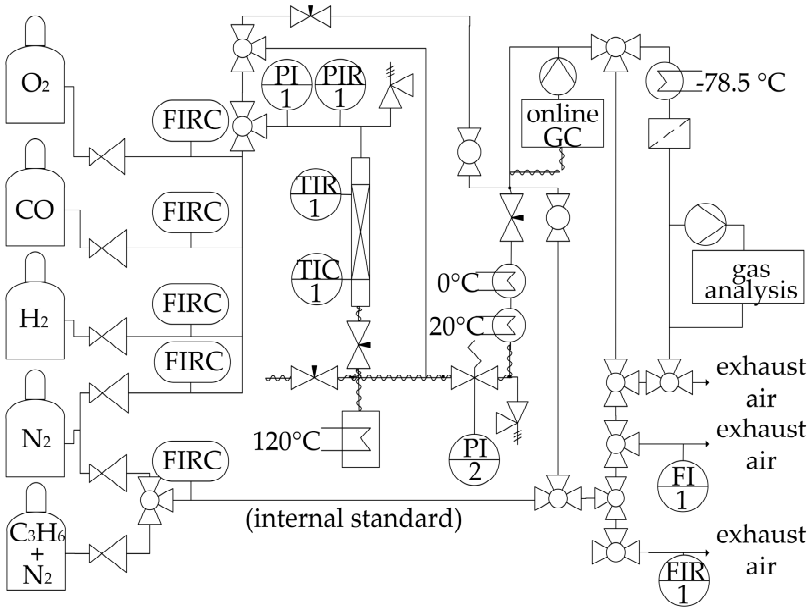

Figure 9. Setup for the FT experiments with a fixed bed reactor.

The catalysts are inhouse-made catalysts containing 10 wt.% cobalt and/or 0.03 wt.% Pt supported on 5 × 5 mm γ-Al_2O_3 particles (Sasol Germany GmbH, Hamburg, Germany). The metals are deposited by wet-impregnation. Therefore, the support is stirred in an aqueous solution of $Co(NO_3)_2 \cdot 6\,H_2O$ (>98%, Carl Roth GmbH + Co. KG, Karlsruhe, Germany) and/or $Pt(NH_3)_4(NO_3)_2$ (Alfa Aesar, Haverhill, MA, USA) in a round-bottomed flask, being part of a rotovap. After applying a reduced pressure of 30 Pa three times to improve the pore filling, the flask is rotated to guarantee homogeneous metal dispersion. The resulting particles are dried at room temperature for at least two days, then calcinated in an air stream heated up in 5 K min^{-1} steps to 360 °C, and then held for 3 h. In Table 3, the characteristics of the catalyst are summarized.

Table 3. Characteristics of the synthesized catalysts used in this work.

Parameter	Co/Pt/Al_2O_3-Catalyst	Co/Al_2O_3-Catalyst	Pt/Al_2O_3-Catalyst
Chemical composition	0.031 wt.% Pt, 10 wt.% Co, rest γ-Al_2O_3	9.7 wt.% Co, rest γ-Al_2O_3	0.03 wt.% Pt, rest γ-Al_2O_3
Size of cylindrical particles	5 × 5 mm	5 × 5 mm	5 × 5 mm
BET surface area	188 $m^2\ g_{Cat}{}^{-1}$	196 $m^2\ g_{Cat}{}^{-1}$	205 $m^2\ g_{Cat}{}^{-1}$
Pore volume	0.36 $cm^3\ g_{Cat}{}^{-1}$	0.4 $cm^3\ g_{Cat}{}^{-1}$	0.43 $cm^3\ g_{Cat}{}^{-1}$
Porosity ε_p	0.53	0.53	0.53

In order to achieve isothermal conditions inside the catalyst bed, the catalyst is diluted with quartz sand (d_p = 250 µm). The mixture is filled in the reactor and after a leak test, the catalyst is activated in 100% H_2 at 360 °C for 16 h. After reduction, the catalyst is cooled to 150 °C; reoxidation is thereby excluded by a gas phase still rich in hydrogen (H_2-to-N_2 ratio of 2). After initiating the FTS reaction by introduction of syngas (here a mixture of CO, H_2, N_2, and traces of O_2), the reactor is heated up to reaction temperature and the temperature is held for at least 100 h to ensure steady state operation. At unsteady state conditions the reaction rate would decrease over time. The cause of the disrobed behavior is the ongoing hydrocarbon filling that builds an increasing diffusion barrier [24]. Afterwards, the parameters such as CO or H_2 concentration, temperature, or pressure were changed individually and held for a further 72 h to observe the effect of each parameter.

3.3. Evaluation of Experimental Data

The CO conversion X_{CO} and O_2 conversion X_{O_2} are calculated according to Equations (5) and (6), respectively,

$$X_{CO} = \frac{\dot{n}_{CO,0} - \dot{n}_{CO}}{\dot{n}_{CO,0}} \tag{5}$$

$$X_{O_2} = \frac{\dot{n}_{O_2,0} - \dot{n}_{O_2}}{\dot{n}_{O_2,0}} \tag{6}$$

with $\dot{n}_i$ as the molar gas flow of component i. $\dot{n}_{i,0}$ and $\dot{n}_i$ is the in- and outgoing molar flow of component i (here O_2 or CO). Based on the CO conversion, the selectivity S for methane and higher hydrocarbons can be determined according to the Equations (7) and (8).

$$S_{CH_4} = \frac{\dot{n}_{CH_4}}{\dot{n}_{CO,0} - \dot{n}_{CO}} \tag{7}$$

$$S_{C_{2+}} = \frac{\dot{n}_{C_{2+}}}{\dot{n}_{CO,0} - \dot{n}_{CO}} \tag{8}$$

The selectivities of O_2 to H_2O and CO_2 (S_{CO_2}, S_{H_2O}) are determined by Equations (9) and (10). For the H_2O selectivity, the selectivity of CO_2 is used since the CO_2 content in the product gas is easily and accurately obtained by online gas analysis.

$$S_{CO_2} = \frac{\dot{n}_{CO_2}}{\dot{n}_{O_2,0} - \dot{n}_{O_2}} \tag{9}$$

$$S_{H_2O} = 1 - S_{CO_2} \tag{10}$$

The reaction rate related to the mass of catalyst is calculated via Equation (11)

$$\dot{r}_i = \frac{\dot{n}_{i,0} - \dot{n}_i}{m_{cat}} \tag{11}$$

where m_{cat} is the mass of the catalyst and $\dot{n}_i$ the molar gas flow of compound i.

4. Conclusions

This work shows that Fischer-Tropsch fixed bed synthesis can be applied with syngas containing traces of O_2 (e.g., about 1%, if syngas is produced in plasma based processes) as long as sufficient cooling of the reactor (tubes) is applied. During FTS with oxygen in the syngas, the catalyst does not oxidize and the O_2 is converted exclusively to H_2O and CO_2. The FTS (acticity of catalyst, product distribution) is not influenced by O_2, except that a small (unwanted, but for the given case unavoidable) consumption of CO and H_2 by reaction with O_2 takes place. The O_2 reaction, i.e., the formation of H_2O and CO_2, is of first order with regard to O_2, and the selectivities to CO_2 (about 30%) and H_2O (70%) are not altered by the O_2 content of the syngas, and also the influence of the CO and H_2 content on the selectivity is marginal.

For the proposed new synthesis route to produce CO_2-neutral maritime fuel via a plasma-based CO supply, the consumption of O_2 leads to an addtional heat release in the FTS, which may be critical with regard to a temperature runaway of a cooled multi-tubular FT reactor: For only 1% O_2 in the syngas, the adiabatic temperature rise is 170 K (compared to about 1500 K for FTS with syngas consisting of pure H_2 and CO in a ratio of 2). To avoid this additional heat release, O_2, if present in the syngas, could be also completely converted to H_2O and CO_2 by a catalytic conversion step and pre-reactor in front of the FT reactor. A similar case is, for example, also discussed and investigated for the removal of oxygen traces present in raw coke oven gas, if high purity H_2 should be produced by pressure swing adsorption. Respective investigations with regard to the case of FTS are currently conducted, and will be presented elsewhere.

Supplementary Materials: The following supporting information can be downloaded at: https://www.mdpi.com/article/10.3390/catal13020391/s1, Figure S1: (a) X-Ray Diffractogram of fresh Co/Pt/Al_2O_3 catalyst. (b) Diffractogram of reduced Co/Pt/Al_2O_3 catalyst. (c) Diffractogram of re-oxidized Co/Pt/Al_2O_3 catalyst., Figure S2: Reduction degree of Co/Al_2O_3 catalyst over time in H_2 atmosphere.

Author Contributions: Conceptualization, A.H.; methodology, A.H.; software, A.H. and C.K.; validation, A.H. and A.J.; formal analysis, A.H. and C.K.; investigation, A.H.; resources, A.J.; writing—original draft preparation, A.H.; writing—review and editing, A.H. and A.J.; visualization, A.H.; supervision, A.J.; project administration, A.J.; funding acquisition, A.J. All authors have read and agreed to the published version of the manuscript.

Funding: This research was funded by the German Federal Ministry for Economic Affairs and Climate Action (Funding code: 03EIV161A-D).

Data Availability Statement: The data presented in this study are available on request from the corresponding author.

Conflicts of Interest: The authors declare no conflict of interest.

Abbreviations

Symbols used	
m (kg)	mass
$\dot{n}$ (mol s^{-1})	molar flow
p (Pa)	pressure
S (-)	selectivity
$\dot{V}$ (m^3 s^{-1})	volumetric flow
X (-)	conversion
Greek symbols	
ε_p (-)	porosity of particle
Sub- and Superscripts	
cat	catalyst
Co	cobalt
i	compound i
Abbreviations	
BET	measurement according to Brunauer-Emmett-Teller
FTS	Fischer-Tropsch synthesis
HC	hydrocarbon
LT-FTS	low temperature Fischer-Tropsch synthesis
MSB	magnetic suspension balance
NTP	normal temperature and pressure (0 °C, 1.013 bar)
PtL	power to liquid

References

1. Jackson, R.B.; Friedlingstein, P.; Andrew, R.M.; Canadell, J.G.; Le Quéré, C.; Peters, G.P. Persistent fossil fuel growth threatens the Paris Agreement and planetary health. *Environ. Res. Lett.* **2019**, *14*, 121001. [CrossRef]
2. Gray, N.; McDonagh, S.; O'Shea, R.; Smyth, B.; Murphy, J.D. Decarbonising ships, planes and trucks: An analysis of suitable low-carbon fuels for the maritime, aviation and haulage sectors. *Adv. Appl. Energy* **2021**, *1*, 100008. [CrossRef]
3. Paraschiv, S.; Paraschiv, L.S. Trends of carbon dioxide (CO_2) emissions from fossil fuels combustion (coal, gas and oil) in the EU member states from 1960 to 2018. *Energy Rep.* **2020**, *6*, 237–242. [CrossRef]
4. Qureshi, F.; Yusuf, M.; Kamyab, H.; Vo, D.-V.N.; Chelliapan, S.; Joo, S.-W.; Vasseghian, Y. Latest eco-friendly avenues on hydrogen production towards a circular bioeconomy: Currents challenges, innovative insights, and future perspectives. *Renew. Sustain. Energy Rev.* **2022**, *168*, 112916. [CrossRef]
5. Schemme, S.; Samsun, R.C.; Peters, R.; Stolten, D. Power-to-fuel as a key to sustainable transport systems–An analysis of diesel fuels produced from CO_2 and renewable electricity. *Fuel* **2017**, *205*, 198–221. [CrossRef]
6. Schmidt, P.; Batteiger, V.; Roth, A.; Weindorf, W.; Raksha, T. Power-to-Liquids as Renewable Fuel Option for Aviation: A Review. *Chem. Ing. Tech.* **2018**, *90*, 127–140. [CrossRef]
7. Qureshi, F.; Yusuf, M.; Kamyab, H.; Zaidi, S.; Junaid Khalil, M.; Arham Khan, M.; Azad Alam, M.; Masood, F.; Bazli, L.; Chelliapan, S.; et al. Current trends in hydrogen production, storage and applications in India: A review. *Sustain. Energy Technol. Assess.* **2022**, *53*, 102677. [CrossRef]
8. König, D.H.; Freiberg, M.; Dietrich, R.-U.; Wörner, A. Techno-economic study of the storage of fluctuating renewable energy in liquid hydrocarbons. *Fuel* **2015**, *159*, 289–297. [CrossRef]
9. van Hoecke, L.; Laffineur, L.; Campe, R.; Perreault, P.; Verbruggen, S.W.; Lenaerts, S. Challenges in the use of hydrogen for maritime applications. *Energy Environ. Sci.* **2021**, *14*, 815–843. [CrossRef]
10. Pearson, R.J.; Eisaman, M.D.; Turner, J.W.G.; Edwards, P.P.; Jiang, Z.; Kuznetsov, V.L.; Littau, K.A.; Di Marco, L.; Taylor, S.R.G. Energy Storage via Carbon-Neutral Fuels Made From CO_2, Water, and Renewable Energy. *Proc. IEEE* **2012**, *100*, 440–460. [CrossRef]
11. Schäppi, R.; Rutz, D.; Dähler, F.; Muroyama, A.; Haueter, P.; Lilliestam, J.; Patt, A.; Furler, P.; Steinfeld, A. Drop-in Fuels from Sunlight and Air. *Nature* **2021**, *601*, 63–68. [CrossRef]
12. Prussi, M.; Scarlat, N.; Acciaro, M.; Kosmas, V. Potential and limiting factors in the use of alternative fuels in the European maritime sector. *J. Clean. Prod.* **2021**, *291*, 125849. [CrossRef] [PubMed]
13. König, D.H.; Baucks, N.; Dietrich, R.-U.; Wörner, A. Simulation and evaluation of a process concept for the generation of synthetic fuel from CO_2 and H_2. *Energy* **2015**, *91*, 833–841. [CrossRef]
14. Kaiser, P.; Pöhlmann, F.; Jess, A. Intrinsic and Effective Kinetics of Cobalt-Catalyzed Fischer-Tropsch Synthesis in View of a Power-to-Liquid Process Based on Renewable Energy. *Chem. Eng. Technol.* **2014**, *37*, 964–972. [CrossRef]
15. Renninger, S.; Stein, J.; Lambarth, M.; Birke, K.P. An optimized reactor for CO_2 splitting in DC atmospheric pressure discharge. *J. CO2 Util.* **2022**, *58*, 101919. [CrossRef]

16. Renninger, S.; Rößner, P.; Stein, J.; Lambarth, M.; Birke, K.P. Towards High Efficiency CO_2 Utilization by Glow Discharge Plasma. *Processes* **2021**, *9*, 2063. [CrossRef]
17. Pöhlmann, F.; Jess, A. Interplay of reaction and pore diffusion during cobalt-catalyzed Fischer–Tropsch synthesis with CO_2-rich syngas. *Catal. Today* **2016**, *275*, 172–182. [CrossRef]
18. Brookes, C.; Bowker, M.; Wells, P. Catalysts for the Selective Oxidation of Methanol. *Catalysts* **2016**, *6*, 92. [CrossRef]
19. Jacobs, G.; Ma, W.; Davis, B. Influence of Reduction Promoters on Stability of Cobalt/g-Alumina Fischer-Tropsch Synthesis Catalysts. *Catalysts* **2014**, *4*, 49–76. [CrossRef]
20. Shiba, N.C.; Liu, X.; Hildebrandt, D.; Yao, Y. Effect of Pre-Treatment Conditions on the Activity and Selectivity of Cobalt-Based Catalysts for CO Hydrogenation. *Reactions* **2021**, *2*, 258–274. [CrossRef]
21. Jahangiri, H.; Bennett, J.; Mahjoubi, P.; Wilson, K.; Gu, S. A review of advanced catalyst development for Fischer–Tropsch synthesis of hydrocarbons from biomass derived syn-gas. *Catal. Sci. Technol.* **2014**, *4*, 2210–2229. [CrossRef]
22. Rößler, S. Akkumulation flüssiger Kohlenwasserstoffe im Porensystem von Kobaltkatalysatoren Während der Anfangsphase der Fischer-Tropsch-Synthese. Ph.D. Thesis, Universität Bayreuth, Bayreuth, Germany, 2019.
23. Bertole, C. The Effect of Water on the Cobalt-Catalyzed Fischer–Tropsch Synthesis. *J. Catal.* **2002**, *210*, 84–96. [CrossRef]
24. Pöhlmann, F.; Kern, C.; Rößler, S.; Jess, A. Accumulation of liquid hydrocarbons in catalyst pores during cobalt-catalyzed Fischer–Tropsch synthesis. *Catal. Sci. Technol.* **2016**, *6*, 6593–6604. [CrossRef]